Journal of Quantitative Spectroscopy & Radiative Transfer 180 (2016) 7–13

Contents lists available at ScienceDirect

Journal of Quantitative Spectroscopy & Radiative Transfer

journal homepage: www.elsevier.com/locate/jqsrt

Journal of
Quantitative
Spectroscopy &
Radiative
Transfer

The band system of ethane around 7 micron: Frequency analysis of the ν_6 band

N. Moazzen-Ahmadi*, J. Norooz Oliaee

Department of Physics and Astronomy, University of Calgary, 2500 University Drive North West, Calgary, Alberta, Canada T2N 1N4

ARTICLE INFO

Article history:
Received 14 February 2016
Received in revised form
28 March 2016
Accepted 29 March 2016
Available online 12 April 2016

Keywords:
Ethane
ν_6 band
Infrared spectrum

ABSTRACT

High quality line parameters of the band systems of ethane are required for accurate characterization of spectral features observed in the atmospheres of Jovian planets and their satellites. To date, experimental characterization of the excited vibrational states lying below 1300 cm^{-1} has been made. This includes the torsional bands around 35 μm, ν_9 (820 cm^{-1}), ν_3 (990 cm^{-1}), $\nu_{12}-\nu_9$ (380 cm^{-1}) and $\nu_9+\nu_4-\nu_4$ (830 cm^{-1}) bands. These earlier high resolution ro-vibrational analyses were made to experimental accuracy. Here, we report a detailed analysis of the weak ν_6 band in the 1340–1410 cm^{-1} region using a spectrum recorded at a resolution of 0.003 cm^{-1} and temperature of 200 K. The Hamiltonian model included couplings between ν_6 and ν_9 (in particular with $\nu_9+2\nu_4$ with which it is resonantly coupled) as well as couplings between ν_6 and ν_8. An excellent fit to within experimental accuracy was obtained. Taking the results of this 5-state fit, together with earlier results on lower lying vibrations, we now have experimental characterization for torsion–vibration states of ethane lying below 1400 cm^{-1}.

1. Introduction

The interest in laboratory spectroscopy of ethane stems from the desire to understand the methane cycle in planetary atmospheres and their moons and the importance of ethane as a trace species in the terrestrial atmosphere. Solar decomposition of methane in the upper part of these atmospheres followed by a series of reactions leads to a variety of hydrocarbon compounds among which ethane is often the second most abundant species [1–7]. Because of its high abundance, ethane spectra have been measured by Voyager and Cassini in the regions around 30, 12, 7, and 3 μm. Therefore, a complete knowledge of line parameters of ethane is crucial for spectroscopic remote sensing of planetary atmospheres.

In Ref. [8], we reported a comprehensive analysis of ethane vibrational states located below 1300 cm^{-1}. As shown in Fig. 1, the torsional states {ground torsional state, $4^1(\nu_4)$, $4^2(2\nu_4)$} were fitted separately (1-state fit, the first block in Fig. 2) [9], while {ground torsional state, $4^1(\nu_4)$, $4^2(2\nu_4)$, $9^1(\nu_9)$, $4^3(3\nu_4)$} was analyzed in a 2-state fit (the first 3×3 blocks in Fig. 2) [10] and {ground torsional state, $4^1(\nu_4)$, $4^2(2\nu_4)$, $9^1(\nu_9)$, $4^3(3\nu_4)$, 3^1, 4^4, 9^14^1, 12^1} was studied in a 4-state fit (the first 6×6 blocks in Fig. 2) [8]. The 1, 2, and 4-state studies were made to within experimental uncertainty. As discussed below, the 5-state analysis reported here uses the entire matrix in Fig. 2 and includes frequencies between or within torsional stacks from five different vibrational states.

Here, we extend the analysis to the 1340–1600 cm^{-1}, shown in the box at the top of Fig. 1. These four levels constitute a complicated manifold with many local and global perturbations. This spectral region corresponds to the excitation of two infrared active fundamentals, ν_6 ~1379 cm^{-1} and ν_8 ~1473 cm^{-1}, and two combination bands, $\nu_9+2\nu_4$

---

* Corresponding author. Tel.: 1 403 220 5394; fax: 1 403 289 3331.
E-mail address: nmoazzen@ucalgary.ca (N. Moazzen-Ahmadi).

http://dx.doi.org/10.1016/j.jqsrt.2016.03.041
0022-4073/© 2016 Elsevier Ltd. All rights reserved.

and $\nu_{12}+\nu_4$. The combination bands do not carry significant infrared intensity but become partially observed through intensity borrowing from the strong ν_8 fundamental. In this work, we focus our attention to the weaker ν_6 parallel band ($\sim$1340–1410 cm^{-1}). A total of 561 lines from the ν_6 band with $0 \le K \le 9$ and $0 \le J \le 30$ were identified and analysed by varying 77 parameters and including a total of 5408 frequencies. The rms deviation of this 5-state fit for the ν_6 band was $37 \times 10^{-5}\ \mathrm{cm}^{-1}$ which is comparable to the experimental uncertainty of $5 \times 10^{-4}\ \mathrm{cm}^{-1}$.

Previous studies of the band system of ethane in the 7 µm region were made by Lattanzi et al. [11,12]. In these analyses the states shown in the box at the top of Fig. 1 were considered as four interacting states but separate from all lower lying torsional and vibrational states which were ignored. For example, the $9^1 4^2$ ($\nu_9+2\nu_4$) was treated as a separate state and not as a member of the torsional stack of 9^1 as is done in the present work. Furthermore, the RMS deviation of the fit in the work by Lattanzi et al. was $3.68 \times 10^{-3}\ \mathrm{cm}^{-1}$ which is more than ten times the experimental uncertainty.

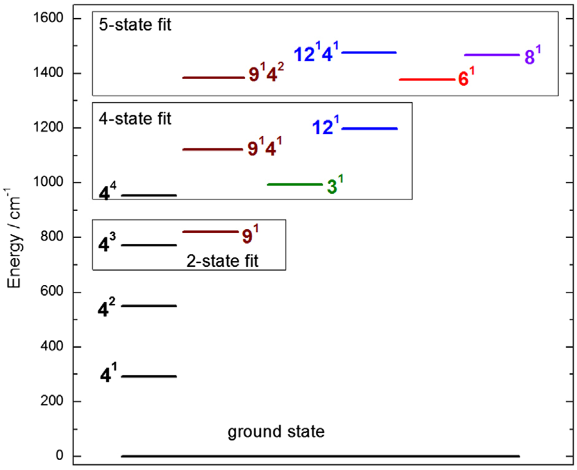

Fig. 1. Vibrational levels of ethane. The four levels in the uppermost enclosed box are the subject of the present paper.

2. Spectra and analysis

A spectrum at a resolution of 0.003 cm^{-1} was recorded using a modified Bomem Fourier transform spectrometer at the National Research Council (NRC) of Canada. The ethane vapor pressure of 80 mTorr at temperature of 200 K was used in a 2 m multiple-traversal gas cell set for a total path of 40 m.

The ν_6 fundamental, whose upper state symmetry is A_{4s}, is an infrared active parallel band, but much weaker than the ν_8 fundamental. A room temperature spectrum of this band is completely dominated by the much stronger lines from the neighboring ν_8 fundamental. This point is well illustrated in Fig. 1 of Ref. [11]. However, in a 200 K spectrum such as that obtained in this work, the ν_6 band is clearly visible. The overview of the spectrum from 1340–1410 cm^{-1} in Fig. 3 shows a clear *Q*-branch around 1379 cm^{-1} and blue shaded *K* structures in both *P*-and *R*-branches. Fig. 4 shows close-up of three potions of the spectrum, one in the *P*-branch (the top trace), one in the central region of the ν_6 band (the middle trace which includes part of the *Q*-branch), and one in the *R*-branch (the bottom trace).

Rotational assignment of the ν_6 band was straight forward. Only lines with $0 \le K \le 9$ had sufficient signal to noise to be included in the fit. In the absence of any perturbations the torsional fine structure is not resolved, indicating that the barrier heights in the ground state and $v_6 = 1$ are not significantly different.

One of the main interactions affecting low values of *K* in ν_6 is the interaction with $\nu_9+2\nu_4$, leading to measurable torsional fine structure for $K=3$, 4, and 5. As can be seen from Fig. 5, the closest approach for $J=15$ is 0.44 cm^{-1} with ($K=4$, $\sigma=0$, $v_6=1$) above its interacting partner (i.e., ($K=3$, $l_9=1$, $\sigma=0$, $v_4=2$, $v_9=1$)) and 1.13 cm^{-1} for ($K=4$, $\sigma=2$, $v_6=1$) which is below its interacting partner (i.e., ($K=3$, $l_9=-1$, $\sigma=2$, $v_4=2$, $v_9=1$)). The fact that ($K=4$, $\sigma=0$, $v_6=1$) and ($K=4$, $\sigma=2$, $v_6=1$) are located on the opposite sides of their interacting levels leads to the largest observed torsional splitting for $K=4$. Here, $\sigma=0, \pm1, \pm2, 3$ labels the torsional sublevels.

A second and much larger Coriolis-type interaction affecting the ν_6 band is with ν_8. For low values of *K*, this

Kg, lg=0	O_{68}, O_{70}	O_{68},O_{70}	O_{71}, O_{72}							
O_{68},O_{70}	Kg+1,l_9=+1	O_{41}				O_{77},O_{78}			O_{74}	
O_{68},O_{70}	O_{41}	Kg-1,l_9=-1		O_{74}		O_{77},O_{78}				
O_{71}, O_{72}			Kg, l_3=0							
		O_{74}		Kg-2,l_{12}=+1	O_{59}					
				O_{59}	Kg-4,l_{12}=-1					
	O_{77},O_{78}	O_{77},O_{78}				Kg,l_6=0	O_{80}, O_{82}	O_{80}, O_{82}		
						O_{80}, O_{82}	Kg+1,l_8=+1			
						O_{80}, O_{82}		Kg-1,l_8=-1		
	O_{74}								Kg+2,l_{12}=-1	O_{59}
									O_{59}	Kg+4,l_{12}=-1

Fig. 2. Hamiltonian matrix used to obtain the total energy. Here, K_g represents the value of *K* for the ground vibrational state. The non-degenerate states are represented by a single block, including the lowest 9 torsional states. The degenerates states are represented by two diagonal blocks each, one for $l_v=+1$ and the other for $l_v=-1$. Each of these blocks also includes 9 torsional states, except for the last two blocks which comprise of the lowest 4 torsional states. The off-diagonal blocks are marked by their torsion mediated intervibrational couplings. See Table 7.